DOI 10.1002/mnfr.200500229 Mol. Nutr. Food Res. 2006, *50*, 314 – 321

New *Monascus* metabolites: Structure elucidation and toxicological properties studied with immortalized human kidney epithelial cells

Anja Knecht, Benedict Cramer and Hans-Ulrich Humpf

Institut für Lebensmittelchemie, Westfälische Wilhelms-Universität Münster, Münster, Germany

Monascus sp. are used for the production of red yeast rice, which has been applied in Asian food and medicine for centuries. The fungi form several secondary metabolites, among others the monascopyridines A and B. We have now detected two new monascopyridines (named C and D) with similar UV absorption spectra and maxima at 306 – 307 nm in red rice fermented with *M. purpureus*. The new monascopyridines have the same chromophores as the already known and differ in a missing γ-lactone ring only. Monascopyridine C has a hexanoyl side chain, whereas monascopyridine D is the higher homologue with an octanoyl side chain. The toxicological properties of monascopyridines were studied using immortalized human kidney epithelial cells, displaying cytotoxic effects in micromolar concentrations with median effective concentration values between 20.7 and 43.2 μmol/L, depending on the compound and method used. The monascopyridines C and D did not induce apoptosis. However, they caused a rise of the mitotic index from 3.21 ± 0.27% (control) to maximum 8.14 ± 0.89% (monascopyridine D) by an accumulation of cells in the metaphase with a simultaneous decrease of cells in the ana- and telophase. Monascopyridine-induced metaphase arrest is caused by a partial or complete loss of the spindle apparatus as indicated by the occurrence of abnormal metaphases and immunological staining of α-tubulin. These effects are indicating an aneuploidic potential and therefore the monascopyridines C and D might contribute to tumor formations.

Keywords: Cytotoxicity / Immortalized human kidney epithelial cells / Monascopyridine / *Monascus* / Red fermented rice / Secondary metabolites

Received: October 31, 2005; revised: December 12, 2005; accepted: December 13, 2005

1 Introduction

Red yeast rice is obtained by the fermentation of rice (*Oryza sativa*) with fungi of the genus *Monascus*, mainly *M. purpureus* and *M. anka*. It has been used in Asia for over 1000 years to color, aromatize and conserve meat, fish and soybean products. It is also applied for medicinal purposes like improved food digestion and blood circulation [1, 2]. Due to its cholesterol lowering properties, red fermented rice has recently gained a lot of interest in the Western countries [3]. Since 1977, the production of *Monascus* pigments in Japan increased from 100 tons a year to 600 tons in 1992 at an estimated value of $ 12 million [4, 5]. Several secondary metabolites have been identified so far, the most important are the six main pigments [6], monacolines [7], monankarines [8], monascodilon [9] and the mycotoxin citrinin [10] (for review see [11]). In 2003, the first *Monascus* metabolites with a pyridine ring, the monascopyridines A and B have been identified in collaboration with our group [12]. However, the pharmacological and toxicological effects of most secondary metabolites are still unknown or unclear [8, 13, 14] and there are even more unidentified metabolites.

Therefore, the aim of this work was to identify further metabolites in red fermented rice and to determine the cytotoxicity and the apoptotic as well as the antimitotic potential in cell culture studies using immortalized human kidney epithelial (IHKE) cells, which have shown a sensitive induction of apoptosis in studies of another *Monascus* metabolite, the mycotoxin citrinin.

Correspondence: Professor Hans-Ulrich Humpf, Institut für Lebensmittelchemie, Westfälische Wilhelms-Universität Münster, Corrensstrasse 45, D-48149 Münster, Germany
E-mail: humpf@uni-muenster.de
Fax: +49-251-83-33-396

Abbreviations: IHKE cells, immortalized human kidney epithelial cells; **AT/PM ratio**, ratio of cells in anaphase + telophase / prometaphase + metaphase; **CY3 conjugated**, carbocyanin 3 conjugated; **HMQC**, heteronuclear multiple quantum correlation; **HMBC**, heteronuclear multiple bond correlation; **NOESY**, nuclear Overhauser effect spectroscopy

2 Materials and methods

2.1 Chemicals

HPLC grade ACN and analytical grade phosphoric acid were from Merck (Darmstadt, Germany). HPLC grade water was prepared with a MilliQ Gradient A10 system (Millipore, Schwalbach, Germany). DMEM/Ham F-12 media, PBS and fetal calf serum were from Biochrom (Berlin, Germany). Accutase™ was purchased from PAA Laboratories (Cölbe, Germany), mouse epidermal growth factor from BD Biosciences (Heidelberg, Germany), goat serum from Gibco BRL (Paisley, UK) and CASY®Ton from Schärfe System (Reutlingen, Germany). The anti-α-tubulin mAb from mouse ascites fluid was from Sigma, CY3-conjugated anti-mouse antibody of the goat from Jackson Immuno Research (Soham, UK). All other chemicals were from Merck and Sigma-Aldrich (Taufkirchen, Germany).

2.2 NMR spectroscopy

^{1}H and 2-D NMR data were acquired in $CDCl_3$ on a Bruker DPX-400 (Bruker BioSpin, Rheinstetten, Germany), ^{13}C-NMR on a Unity plus (Varian, Palo Alto, CA, USA) NMR spectrometer. For structural elucidation and NMR signal assignment 2-D NMR experiments, such as double-quantum filtered correlated spectroscopy (DQF-COSY), heteronuclear multiple quantum correlation (HMQC), heteronuclear multiple bond correlation (HMBC), and 2-D nuclear Overhauser effect spectroscopy (NOESY) were carried out. Puls programs were taken from the Bruker software library.

2.3 Exact mass measurements

Mass spectra were recorded on a Quattro-LC instrument (Waters-Micromass, Manchester, UK). Substances were dissolved in MeOH/$CHCl_3$.

2.4 Preparation of red fermented rice

The strain *Monascus purpureus* (DSM 1603) was obtained from the German Collection of Microorganisms and Cell Cultures (DSMZ, Braunschweig, Germany). It was cultured as described in reference [12] with slight modifications. Briefly, it was cultured on a rich rice medium consisting of the autoclaved mixture of 20 g ground rice, 8 g sucrose, 2 g yeast extract, 0.1 g KH_2PO_4, 0.1 g $CaCl_2$ and 0.5 g $MgSO_4$ in 100 mL of water [15] in Petri dishes for 3 weeks at 30°C. The fermented rice was dried at 30°C and subsequently pulverized.

2.5 HPLC analysis

A Jasco PU-2089 low pressure pump, autosampler AS-2057 plus and an MP-201 plus diode array detector combined with Borwin PDA 1.5 software (Jasco, Grossumstadt, Germany) were used. RP HPLC was run on a 250 × 4 mm id ReproSilPur C18-AQ column (Fa. Maisch, Ammerbach, Germany) with a gradient of (A) 0.25 M phosphoric acid and ACN (1 : 1) and (B) ACN: 0–12 min 100% A, 20 min 20% A, 22 min 20% A, 28 min 100% A, 30 min 100% A; flow: 0–5 min: 0.7–0.8 mL/min, 5–12 min: 0.8–1 mL/min, 12–30 min: 1 mL/min. Chromatograms were recorded between 200 and 600 nm, which allowed differentiating and assigning of the peaks of monascopyridine C (**1**) and D (**3**) by comparing them to references of monascopyridine A (**4**) and B (**6**).

2.6 Isolation of monascopyridine C and D

Aliquots of 0.5 g of the pulverized fermented rice (see Section 2.4) were extracted with 1.5 mL of a mixture of 0.25 M phosphoric acid and ACN (1 : 1) in an ultrasound water bath and subsequently centrifuged (12 000 × g, 5 min, 15°C). The supernatant was directly used for HPLC separation. Extracts were fractionated by HPLC on a 250 × 16 mm id Eurospher-100 C18 column (Knauer GmbH, Berlin, Germany) using the following gradient of (A) 0.25 M phosphoric acid and ACN (1 : 1) and (B) ACN: 0–10 min 100% A, 60 min 20% A, 70 min 20% A, 80 min 100% A, 90 min 100% A; flow: 3 mL/min. Fractions eluting at 21–23 min (**1**) and 36–38 min (**3**) were further fractionated using an (A) ACN and (B) water gradient on the same column: 0–5 min 100% A, 11 min 65% A, 15 min 65% A, 35 min 0% A, 45 min 0% A, 55 min 100% A, 65 min 100% A; flow: 3 mL/min. **1** eluted at 33.2 min, **3** at 53.0 min. Similar to the monascopyridines A and B [12], both compounds had absorption maxima at 306–307 nm and were obtained as colorless needles after removal of solvents and recrystallization from ethanol.

2.7 Monascopyridine C

^{1}H NMR (400 MHz, 25°C, $CDCl_3$,) δ 0.9 (t, J = 6.8 Hz, 3H; CH_3; H-24), 1.23 (s, 3H; CH_3; H-18), 1.24–1.36 (m, 4H; CH_2; H-22, H-23), 1.55–1.65 (m, 2H; CH_2; H-21), 1.99 (dd, J = 6.9, 1.6 Hz, 1H; CH_3; H-13), 2.41–2.47 (m, 1H; CH_2; H-14a), 2.48 (t, J = 7.5 Hz, 2H; CH_2; H-20), 2.62 (ddd, J = 17.5, 12.1, 0.9 Hz, 1H; CH_2; H-5a), 2.72–2.79 (m, 1H; CH; H-6), 3.11 (dd, J = 17.1, 2.8 Hz, 1H; CH_2; H14b), 3.19 (dd, J = 17.5, 4.6 Hz, 1H; CH_2; H-5b), 6.52 (dd, J = 15.4, 1.6 Hz, 1H; CH; H-11), 6.98 (dq, J = 15.4, 6.9 Hz, 1H; CH; H-12), 7.02 (s, 1H; CH; H-3), 9.09 (s, 1H; CH; H-10); ^{13}C NMR (150 MHz, $CDCl_3$) δ 209.7 (C-15), 200.5 (C-8), 160.0 (C-2), 151.0 (C-10), 150.2 (C-4), 135.2 (C-12), 130.5 (C-11), 123.2 (C-9), 119.9 (C-3), 75.0 (C-7), 43.3 (C-20), 41.9 (C-14), 39.1 (C-6), 32.7 (C-5), 31.4 (C-22), 23.6 (C-21), 22.5 (C-23), 19.2 (C-18), 18.7 (C-13), 13.6 (C-24). ESI-MS/MS of *m/z* 330 (34 eV): 173 (48), 216 (100), 312 (30), 330 (35). ESI-HRMS: *m/z* 330,2084 $[M + H]^+$ (calculated for $[M + H]^+$ 330,2069)

2.8 Monascopyridine D

^{1}H NMR (400 MHz, 25°C, $CDCl_3$) δ 0.88 (s, J = 7.1 Hz, 3H; CH_3; H-26), 1.23 (s, 3H; CH; H-18), 1.24–1.33 (m, 8H; CH_2; H-22–H-25), 1.55–1.65 (m, 2H; CH_2; H-21), 1.99 (dd, J = 6.9, 1.6 Hz, 1H; CH_3; H-13), 2.41–2.47 (m, 1H; CH_2; H-14a), 2.48 (t, J = 7.5 Hz, 2H; CH_2; H-20), 2.62 (ddd, J = 17.5, 12.1, 0.9 Hz, 1H; CH_2; H-5a), 2.70–2.77 (m, 1H; CH; H-6), 3.11 (dd, J = 17.1, 2.8 Hz, 1H; CH_2; H-14b), 3.19 (dd, J = 17.5, 4.6 Hz, 1H; CH_2; H-5b), 6.52 (dd, J = 15.4, 1.6 Hz, 1H; CH; H-11), 6.98 (dq, J = 15.4, 6.9 Hz, 1H; CH; H-12), 7.01 (s, 1H; CH; H-3), 9.09 (s, 1H; CH; H-10); ^{13}C NMR (150 MHz, $CDCl_3$) δ 209.9 (C-15), 200.5 (C-8), 160.0 (C-2), 150.2 (C-4), 150.0 (C-10), 135.5 (C-12), 130.3 (C-11), 123.2 (C-9), 119.9 (C-3), 75.0 (C-7), 43.3 (C-20), 41.7 (C-14), 38.9 (C-6), 32.8 (C-5), 31.7 (C-24), 29.7 (C-23), 29.0 (C-22), 23.9 (C-21), 22.6 (C-25), 19.1 (C-18), 18.6 (C-13), 14.1 (C-26). ESI-MS/MS of *m/z* 358 (37 eV): 173 (25), 216 (100), 340 (30), 358 (38). ESI-HRMS: *m/z* 358,2406 $[M + H]^+$ (calculated for $[M + H]^+$ 358,2382).

2.9 Cell culture

Immortalized human kidney epithelial cells (IHKE cells, passage 150–180) were kindly provided by M. Gekle (Würzburg, Germany). They were cultured as described by Tveito *et al*. [16] in DMEM/Ham's-F12 medium (100 µL/cm^2) enriched with 13 mmol/L $NaHCO_3$, 15 mmol/L HEPES, 36 µg/L hydrocortisone, 5 mg/L human apotransferrin, 5 mg/L bovine insulin, 10 µg/L mouse epidermal growth factor, 5 µg/L sodium selenit, 10% fetal calf serum and in addition 1% penicillin/streptomycin under standard cell culture conditions (37°C, 5% CO_2).

To exclude any binding of the tested compounds to serum proteins, cytotoxicity assays were carried out in serum-free medium. Under these conditions, cells were still proliferating, as determined with electronic cell counting. The control cells and the cells incubated with the test compounds were treated with the same amount (<1%) of organic solvent (ACN/0.25 M H_3PO_4).

2.10 Cytotoxicity assay

2.10.1 CCK8 assay

The determination of the cytotoxicity by measuring the metabolic activity of the cells in the CCK8 assay was carried out as described recently [17] with an incubation time of 24 h. Results are presented as mean values from three replicate experiments with different passages enclosing ten wells each.

2.10.2 Electronic cell counting

For electronic cell counting, a CASY® TT cell counter (Schärfe System) was used. Approximately 6×10^4 cells were seeded in Petri dishes (∅ 30 mm) and cultivated for 48 h. Afterwards they were cultured for 24 h in serum-free medium and then incubated for 24 h with the test compounds. After incubation, cell medium was collected; adherent cells were harvested by incubating with Accutase™ for 15 min, combined with the previously collected cell medium and centrifuged subsequently (120 × g, 5 min, 20°C). The pellet was resuspended in 1 mL PBS and 200 µL of this suspension was mixed with 10 mL CASY®-Ton for measurement. Viability was calculated as the percentage of viable cells to the total number of cells. The viability of the treated cells was compared to the viability of an untreated control. Results are presented as mean values from two replicate experiments with different passages enclosing three Petri dishes each.

2.11 Caspase 3 assay

Before incubation with the substances, approximately 5×10^6 cells were incubated in serum-free medium for 24 h in Petri dishes. Chemicals were incubated for 12, 24 and 48 h, respectively. Caspase 3 activity was measured according to the manufacturer's instruction (Clontech Laboratories GmbH, Heidelberg, Germany) with slight modifications. In brief, cells were washed with PBS once, incubated with 100 µL cell lysis buffer for 30 min on ice, harvested and centrifuged (13 000 × g, 10 min, 4°C). Supernatant was incubated with the caspase 3 substrate N-Acetyl-Asp-Glu-Val-Asp-7-amino-4-trifluoromethylcoumarin (25 µmol/L end concentration) for 60 min at 37°C and fluorescence of the cleaved product was measured at 405 nm excitation and 520 nm emission wavelength in a microtiter-plate-reader (FLUOstar Optima, BMG LABTECH GmbH, Offenbach, Germany). Cleaved 7-amino-4-trifluoromethylcoumarin (AFC) was quantified by a calibration curve using known AFC concentrations. The protein content was determined with a bicinchoninic acid assay kit from Sigma. Results are presented as mean values from three replicate experiments with different passages enclosing three Petri dishes each.

2.12 DNA ladder formation

Before incubation with the substances, approximately 8×10^6 cells were incubated in serum-free medium for 24 h in Petri dishes. Chemicals were incubated for 48 h. Culture medium was collected and cells were separated by centrifugation (500 × g, 5 min, 4°C). Seeded cells were harvested in cell lysis buffer (10 mM TRIS-HCl, 150 mM NaCl, 2 mM EDTA, 1% SDS, adjusted to pH 8.0 + 0.5 mM guanidin hydrochloride), incubated on ice together with the previously obtained cell pellet and centrifuged (20 000 × g, 15 min, 4°C). RNase (30 µg/mL) and Proteinase K (60 µg/mL) were added to the supernatant successively, incubated for 30 min each and centrifuged (20 000 × g, 15 min, 4°C). DNA was extracted by using a DNA-Wizard Clean-up-Kit (Promega GmbH, Mannheim, Germany) according to the

manufacturer's instruction. DNA ladder formation was analyzed in 1.5% agarose gel.

2.13 Determination of the antimitotic potential and detection of apoptotic bodies

As a positive control with known spindle poisoning potential, colchicine was used [18]. Incubation of the cells was carried out on sterile microscope slides. Before applying the substances, $5-8 \times 10^4$ cells per slide were grown for 48 h. Substances were incubated for 24 h. Cells were fixed by storing the slides in a mixture of methanol and glacial acetic acid (3+1) at −20°C for at least 12 h. Cell DNA was colored by incubating the cells in a methanolic solution of Hoechst 33258 (10 µg/mL) for 20 min. For reduction of the background fluorescence, slides were washed briefly with PBS buffer. As a parameter of mitotic arresting activity, the mitotic index was determined by counting at least 1000 cells per slide on an Axiovert 25 CFL fluorescence microscope (Carl Zeiss, Jena, Germany) with an excitation wavelength of 365 nm and emission at 420 nm. The different mitotic phases were distinguished. For calculating the mitotic index, all mitotic phases were added and the results are given as percentage fraction of all cells. Cells in prometa- and metaphase were further divided into normal prometa- and metaphases and cells with structural damages – such as c-mitosis –, dislocated chromosomes and multipolar spindles. The different metaphases were classified as percentage fraction of all prometa- and metaphases. As an additional index of mitotic arresting activity, the ratio of cells in ana- and telophase to cells in prometa- and metaphase was calculated (AT/PM ratio). Results are presented as mean values of three replicate experiments with different passages enclosing two slides each. In the same manner, apoptotic bodies can be detected.

2.14 Immunological staining of the mitotic spindles

Cells were cultured and incubated as described in Section 2.13. Cells were fixed in formaldehyde solution (3.5 g paraformaldehyde was suspended in 50 mL H_2O, mixed with 1 mL 1 M NaOH and heated at 60°C for 5 min). This solution was mixed with the same volume $2 \times$ CB buffer (137 mM NaCl, 5 mM KCl, 1.1 mM Na_2HPO_4, 0.4 mM KH_2PO_4, 2 mM $MgCl_2$, 2 mM EDTA, 5 mM PIPES, 5.5 mM glucose in demineralized water) and adjusted to pH 6.1. Then 0.25 % triton X-100 were added for 5 min and then stored in methanol (−20°C) for at least 30 min. The slides were washed (three times, 5 min) with PBS-CMF buffer (137 mM NaCl, 2.7 mM KCl, 7.8 mM Na_2HPO_4 and 1.5 mM KH_2PO_4 in demineralized water; adjusted to pH 8.0) and incubated with goat serum for 1 h (37°C). Then cells were washed in PBS-CMF once and incubated with the primary antibody (anti-α-tubulin mAb from mouse ascites fluid, diluted 1 : 500 with 1% BSA solution) for 1 h (37°C). Cells were washed again (three times, 5 min) and then incubated for 1.5 h (37°C) with the secondary antibody (anti-mouse antibody of the goat, CY3 conjugated, diluted 1 : 250 with 1% BSA solution). Then cells were washed (three times, 5 min), stained with Hoechst 33258 as described in Section 2.13 and covered with mounting media (PBS mixed with glycerin 1 : 1 v/v plus 0.1% ascorbic acid). Cells were viewed with two different filters: Hoechst staining was viewed as stated in Section 2.13, mitotic spindles were observed with an excitation wavelength of 546 nm and emission at 590 nm.

2.15 Data analysis

Data are represented as means ± SD. The *n*-value is given in the figures and equals the number of wells, Petri dishes or slides used for the measurements. The median effective concentration (EC_{50}) values were calculated using SigmaPlot 8.0. Statistical significance of changes of the mitotic index and AT/PM ratio were determined by unpaired Student's *t*-test. Differences were considered as statistically significant when $p = 0.01$.

3 Results and discussion

As a representative example, Fig. 1 shows an HPLC chromatogram of red fermented rice obtained from *M. purpureus* (DSM 1603) grown on rich rice medium. In addition to the already known monascopyridines A and B (**4** and **6** in Fig. 1), we detected two new substances with the same UV absorption spectra eluting at 5.9 and 11.4 min, which were numbered **1** and **3**. The *M. purpureus* strain DSM 1603 also

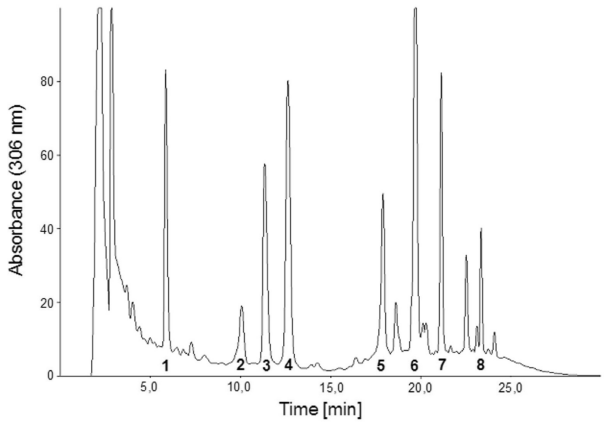

Figure 1. HPLC chromatogram of red fermented rice obtained from *M. purpureus* (DSM 1603) grown on rich rice medium: **1**. monascopyridine C, **2**. rubropunctamine, **3**. monascopyridine D, **4**. monascopyridine A, **5**. monascorubramine, **6**. monascopyridine B, **7**. monascin, **8**. ankaflavin. λ = 306 nm (for structures see Figs. 2 and 3).

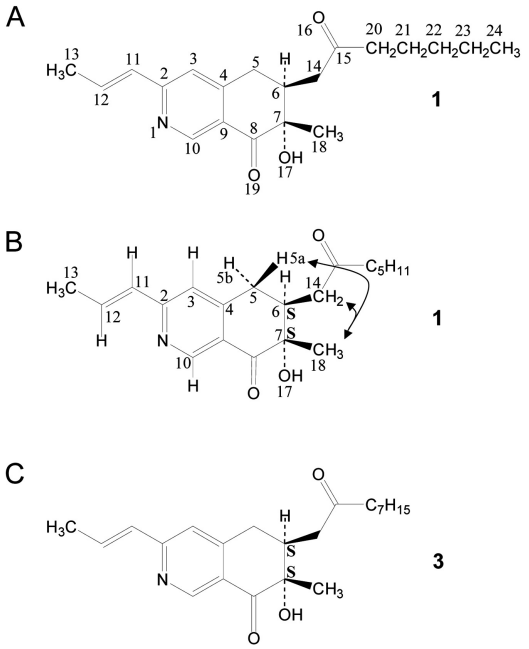

Figure 2. (A) Structure of monascopyridine C (**1**) and numbering system. (B) NOESY responses indicating proximities in monascopyridine C (**1**). (C) Structure of monascopyridine D (**3**).

produced the red pigments rubropunctamine (**2**) and monascorubramine (**4**), as well as the yellow compounds monascin (**7**) and ankaflavin (**8**) (see Fig. 3). The compounds were identified by comparison of their retention times and UV-Vis absorption spectra with reference compounds. Both new secondary metabolites **1** and **3** were isolated by preparative HPLC.

Compound **1**, which was named monascopyridine C, displayed an exact mass corresponding to the molecular formula $C_{20}H_{27}NO_3$. The UV absorption spectrum was almost identical with the spectra of monascopyridine A and B indicating the presence of the same chromophore. This was confirmed by NMR data. For structure elucidation ^1H, ^{13}C, $^1H,^1H$-COSY, $^1H,^{13}C$-HMBC, $^1H,^{13}C$-HMQC and $^1H,^1H$-NOESY spectra were recorded (for details and data see Sections 2.2 and 2.7). The structure of **1** is shown in Fig. 2A. The absolute configuration was deduced from coupling constants and $^1H,^1H$-NOESY-experiments. The responses obtained from the NOESY spectra of **1** are shown in Fig. 2B. NOESY signals were detected for H-5a/H-18, H-14a/H-18 and H-14b/H-18. This can be explained by the steric properties of the non-aromatic ring in which the H-18 methyl group, the proton H-5a and the methylene group H-14 are on the same side. Additionally, the coupling constants between H-5a/H-6 and H-5b/H-6 respectively, show that H-5b and H-6 are on the same side.

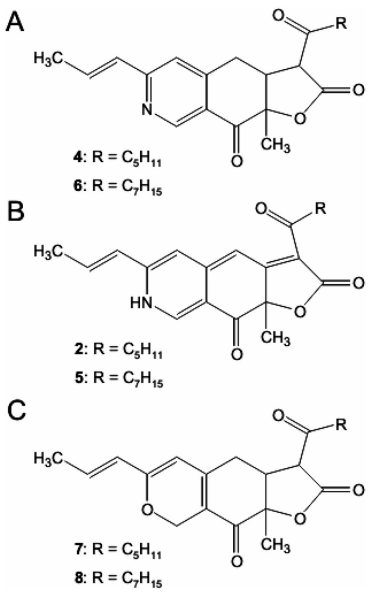

Figure 3. Structure of (A) monascopyridine A (**4**) and B (**6**), (B) rubropunctamine (**2**) and monascorubramine (**5**), (C) monascin (**7**) and ankaflavin (**8**).

The exact mass of compound **3**, named monascopyridine D, revealed the molecular formula $C_{22}H_{31}NO_3$, suggesting two additional methylene groups. From the 1-D- and 2-D NMR spectra we elucidated the structure shown in Fig. 2C with a C_7H_{15} octanoyl side chain instead of C_5H_{11} (Fig. 2C). The same arrangement in pairs of compounds with hexanoyl and octanoyl side chains was also found for the monascopyridines A and B (**4**, **6**) as well as for the pigments of *Monascus* (see Fig. 3) [11, 12]. The structural difference between the new and the known monascopyridines is the missing lactone ring in **1** and **3**, so the biosynthetic pathway of the four monascopyridines seems to be similar. However, the biosynthesis is not known yet, but as the **4** and **6** are formally dehydrogenated derivates of the red pigments **2** and **5** (Fig. 3A and B) their biosynthesis is probably coupled with the pathway of the pigments [12].

To determine the cytotoxicity and the apoptotic as well as the antimitotic potential of the new secondary metabolites, cell culture experiments using IHKE cells were performed. The monascopyridines C and D caused a reduction of the metabolic activity (Fig. 4A) and of the cell viability (Fig. 4B) in IHKE cells in micromolar concentrations. As shown in Table 1, there was only little difference between the EC_{50} values obtained with colorimetrical endpoint detection (CCK8-assay) and electronic cell counting. The more lipophilic compound monascopyridine D was slightly more cytotoxic than monascopyridine C. Cell viability measured with the CCK8 assay was reduced to approximately 58% of the untreated control (Fig. 4A). When using electronic cell counting, the reduction of the percentage of

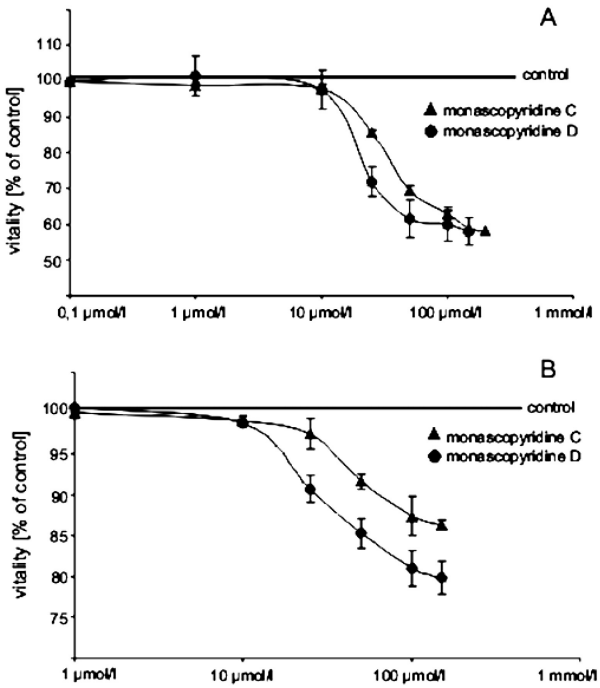

Figure 4. Cytotoxicity of monascopyridine C (**1**) and D (**3**) with (A) colorimetrical endpoint detection (CCK8 assay) and (B) electronic cell counting. IHKE cells were incubated for 24 h with **1** and **3** in concentrations of (A) 0.1 – 200 µmol/L and (B) 1 – 150 µmol/L [$n = 30$ (A), $n = 6$ (B), mean ± SD].

Table 1. EC_{50} values of the monascopyridines in IHKE cells[a)]

Substance	EC_{50} CCK8-assay (µmol/L)	EC_{50} cell counting (µmol/L)
Monascopyridine C	35.4 ± 1.5	43.2 ± 1.3
Monascopyridine D	20.7 ± 1.3	27.0 ± 1.3

a) EC_{50} median effective concentration; (24-h incubation, for details see Section 2.10).

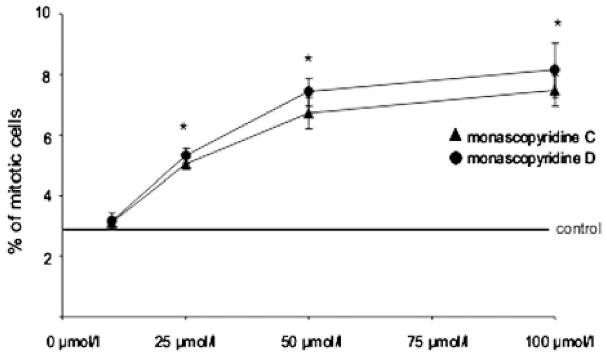

Figure 5. Mitotic arresting activity expressed as the mitotic index in % of IHKE cells after 24 h of incubation with **1** and **3**. Mitotic index of the control: 3.21 ± 0.27%; mitotic index of the positive control colchicine at 25 nmol/L: 24.15 ± 1.79% ($n = 6$, mean ± SD). * Indicates significant difference from control ($p = 0.01$).

vital cells was even lower with values of 80% compared to the control for monascopyridine D and 86% for monascopyridine C (Fig. 4B).

Apoptosis, in contrast to necrotic cell death, is characterized by DNA cleavage, cytosolic as well as nuclear shrinkage and the occurrence of apoptotic bodies without breakdown of the plasma membrane. These morphological characteristics are attributed to the activation of cysteine proteases, the so-called caspases [19]. Caspase 3 activity – as a marker for apoptosis – can be measured specifically by using the substrate (N-Acetyl-Asp-Glu-Val-Asp-7-amino-4-trifluoromethylcoumarin), from which the fluorogenic compound AFC (7-amino-4-trifluoromethylcoumarin) is released. Other classical biochemical markers are the presence of oligonucleosome-sized fragments of DNA, leading to the typical DNA ladder when analyzed by agarose gel electrophoresis, and the occurrence of apoptotic blebs, which can be observed after visualizing the nuclear DNA with fluorogenic substances like bisbenzimide [20].

To study the caspase 3 activity of IHKE cells under the influence of monascopyridines, cells were incubated for 24 h with 1, 10, 25 and 50 µmol/L, and for 12 and 48 h with 50 µmol/L only. The monascopyridines did not show any activation of the caspase 3 in the tested concentrations during the incubation times ranging from 12 to 48 h (data not shown). In addition, no DNA ladder appeared after incubation with 50 µmol/L for 48 h (data not shown). When detecting mitotic cells after incubating for 24 h (see discussion below), only cells treated with 25 nmol/L colchicine formed apoptotic bodies. Therefore, it can be concluded that the monascopyridines C and D have no apoptotic potential within the concentrations tested.

If cells are damaged, they are unable to pass the cell-cycle control points and proceed to the next phase. One control point is placed during mitosis at the transition from meta- to anaphase, where the spindle microtubule structure, the chromosome alignment and their attachment to the kinetochores are checked [21]. If the function of the kinetochores or the spindle is affected, cells accumulate in the metaphase (metaphase-arrest) [22].

As shown in Fig. 5, monascopyridines C and D in concentrations higher than 25 µmol/L cause a significant increase of the mitotic index from 3.21 ± 0.27% (control) to 7.47 ± 0.50% for monascopyridine C and to 8.14 ± 0.89% for monascopyridine D. The significant decrease of the AT/PM ratio (Fig. 6) from 0.48 ± 0.027 (control) to 0.027 ± 0.009 (100 µmol/L) for monascopyridine C and 0.026 ± 0.010 (100 µmol/L) for monascopyridine D, respectively, also

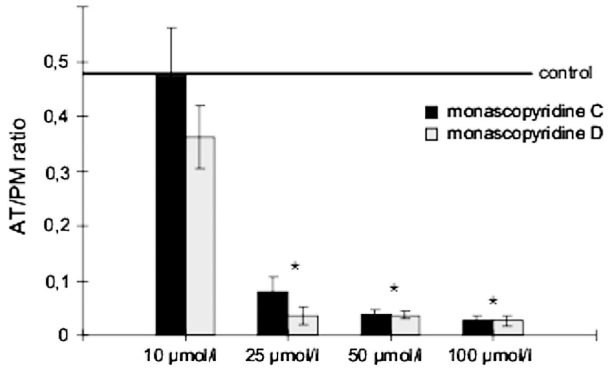

Figure 6. AT/PM ratio (proportion of anaphases plus telophases to prometa- and metaphases) evaluated for the monascopyridines C (**1**) and D (**3**) after incubation of IHKE cells for 24 h. AT/PM ratio of the control: 0.48 ± 0.03 AT/PM, ratio of the positive control colchicine at 25 nmol/L: 0.00 ($n = 6$, mean ± SD). * Indicates significant difference from control ($p = 0.01$).

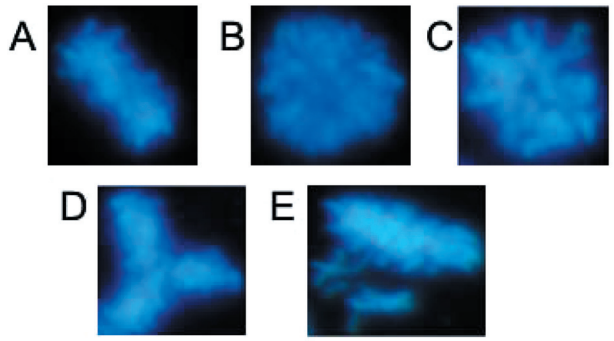

Figure 7. Fluorescent microscopic photographs of IHKE cells (24-h incubation) stained with bisbenzimide (Hoechst 33258). (A) Normal metaphase of control cells, (B) c-Mitosis induced with 25 nmol/L colchicines, (C – E) Examples of aberrant metaphases induced by monascopyridines (50 µmol/L **3**) (C) c-mitosis, (D) tripolar spindle, (E) dislocated chromosomes.

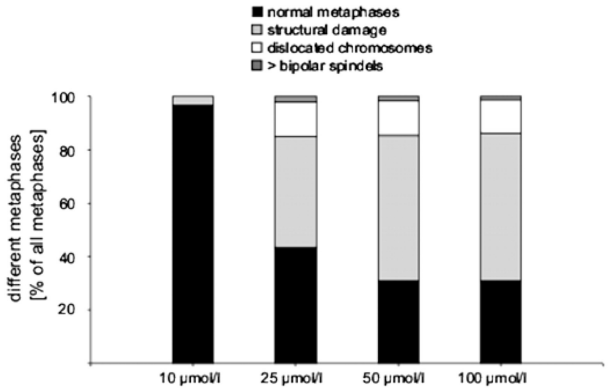

Figure 8. Percentage of normal and the different abnormal metaphases after 24- h incubation of IHKE cells with monascopyridine C (**1**). Percentage of abnormal metaphases of the control: 0%; percentage of aberrant metaphases of the positive control colchicine at 25 nmol/L: 95% ($n = 6$).

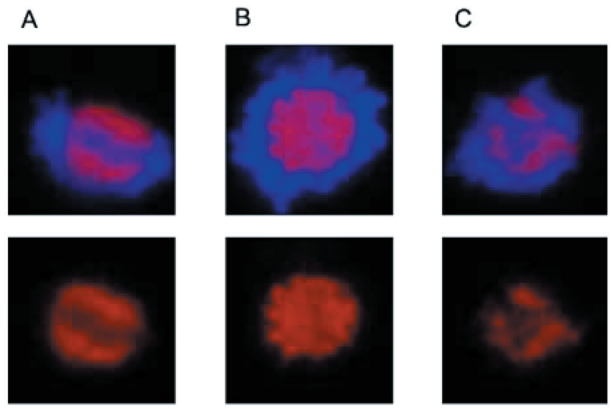

Figure 9. Overlapping of bisbenzimide-stained DNA and CY3-immunologically stained α-tubulin (above) and tubulin spindles (below). (A) Control, (B) 50 µmol/L monascopyridine C (**1**), (C) 50 µmol/L monascopyridine D (**3**) (IHKE cells, 24-h incubation).

shows that the monascopyridines C and D inhibit the mitosis in the metaphase without a complete stop of mitosis as a few cells could still proceed to the ana- and telophase. The monascopyridine-induced metaphase arrest is caused by a partial or complete loss of the spindle apparatus as indicated by the occurrence of abnormal metaphases. They consist of c-mitoses and dislocated chromosomes mainly, which appear with the spindle poison colchicine. As shown in Fig. 7B and C, c-mitosis induced by the monascopyridines is similar to the effect of colchicine. The appearance of monascopyridine induced c-mitosis remained almost constant between concentrations of 25 and 100 µmol/L.

Both monascopyridines lead to similar aberrant mitotic figures shown in Fig. 7C – E. As a representative example, Fig. 8 shows the effect of monascopyridine C on the nuclear profile of IHKE cells undergoing mitosis after 24-h incubation. With increasing concentrations, the number of structural damages increases and varies between 69 and 73% of all cells with 100 µmol/L monascopyridine C and monascopyridine D, respectively. The number of cells with unattached chromosomes remains constant at about 13% between 25 and 100 µmol/L, whereas the number of cells with multipolar spindles reaches its maximum (with 2 – 4%) at 25 µmol/L. The dose-dependent increase in aberrant metaphases is another evidence for the metaphase arresting activity already shown by the increase of the mitotic index and the decrease of the AT/PM ratio.

The mechanistic assumption of the interference with the mitotic spindle was confirmed by immunological staining of α-tubulin, which showed changed tubulin assembly up to its complete disappearance. This effect also occurs in cells treated with colchicine, which is known to bind to the tubu-

lin and therefore prevents regular spindle assembly [18]. As shown in Fig. 9, the normal spindle assembly is changed (Fig. 9B) and begins to disappear (Fig. 9C). These effects occur with both compounds, so the monascopyridines cause mitotic arrest and c-mitosis by damaging the mitotic spindle.

4 Concluding remarks

The monascopyridines C and D prevent cells from normal mitosis by arresting them in the metaphase through interaction with the mitotic spindle. The interaction of substances with spindle microtubuli contribute to spindle malfunction, so it is conceivable that changes in the microtubule properties could lead to chromosome missegregation and aneuploidy [23, 24]. Although there is no direct link between defects in the mitotic machinery and aneuploidy in cancer, there is strong evidence that supports the notion that aneuploidy in cancer develops in most cases from persistent missegregation of chromosomes in mitosis [24, 25]. Concerning the monascopyridines C and D, no data about their bioavailability are existing at present, so the effect of these compounds on the human health cannot be judged finally. However, the observed interference of the monascopyridines with cell division is currently an indication that the use of red rice in human nutrition seems critical. This is also supported by the fact that the toxicological effects of many other secondary metabolites of *Monascus* are still unknown.

We thank D. Wild for samples of Monascus metabolites and for helpful discussions, H. Luftmann for mass measurements, S. Klumpp for the opportunity of fluorescence microscopy, L. Lehmann for the gift of antibodies and goat serum and M. Gekle for providing IHKE cells.

5 References

[1] Ma, J., Li, Y., Ye, Q., Li, J., *et al.*, *J. Agric. Food Chem*. 2000, *48*, 5220 – 5225.

[2] Mudgett, R. E., *Nat. Food Color* 2000, *14*, 31 – 85.

[3] Heber, D., Yip, I., Ashley, J. M., Elashoff, D. A., *et al.*, *Am. J. Clin. Nutr*. 1999, *69*, 231 – 236.

[4] Sweeny, J. G., Estrada-Valdes, M. C., Iacobucci, G. A., Sato, H., Sakamura, S., *J. Agric. Food Chem*. 1981, *29*, 1189 – 1193.

[5] Lee, Y.-K., Chen, D.-C., Chauvatcharin, S., Seki, T., Yoshida, T., *J. Ferment. Bioeng.* 1995, *79*, 516 – 518.

[6] Blanc, P. J., Loret, M. O., Santerre, A. L., Pareilleux, A., *et al.*, *J. Food Sci*. 1994, *59*, 862 – 865.

[7] Endo, A., Komagata, D., Shimada, H., Monacolin, M., *J. Antibiot*. 1986, *39*, 1670 – 1673.

[8] Hossain, C. F., Okuyama, E., Yamazaki, M., *Chem. Pharm. Bull*. 1996, *44*, 1535 – 1539.

[9] Wild, D., Toth, G., Humpf, H.-U., *J. Agric. Food Chem*. 2002, *50*, 3999 – 4002.

[10] Blanc, P. J., Laussac, J. P., Le Bars, J., Le Bars, P., *et al.*, *Int. J. Food Microbiol*. 1995, *27*, 201 – 213.

[11] Jůzlová, P., Martínková, L., Křen, V., *J. Industr. Microbiol*. 1996, *16*, 163 – 170.

[12] Wild, D., Toth, G., Humpf, H.-U., *J. Agric. Food Chem*. 2003, *51*, 5493 – 5496.

[13] Martínková, L., Jůzlová, P., Veselý, D., *J. Appl. Bact.* 1995, *79*, 609 – 616.

[14] Martínková, L., Patáková-Jůzlová, P., Křen, V., Kučerová, Z., *et al.*, *Food Add. Contam*. 1999, *16*, 15 – 24.

[15] Fink-Gremmels, J., Dresel, J., Leistner, L., *Fleischwirtsch*. 1991, *71*, 1184 – 1186.

[16] Tveito, G., Hansteen, I., Dalen, H., Haugen, A., *Cancer Res*. 1989, *49*, 1829 – 1835.

[17] Bretz, M., Knecht, A., Göckler, S., Humpf, H.-U., *Mol. Nutr. Food Res*. 2005, *49*, 306 – 316.

[18] Jordan, A., Hadfield, J. A., Lawrence, N. J., McGown, A. T., *Med. Res. Rev.* 1998, *18*, 259 – 296.

[19] Edinger, A. L., Thompson, C. B., *Curr. Opin. Cell Biol*. 2004, *16*, 663 – 669.

[20] Schwerdt, G., Freudinger, R., Mildenberger, S., Silbernagl, S., Gekle, M., *Cell Biol. Toxicol*. 1999, *15*, 405 – 415.

[22] Steward, Z. A., Pietenpol, J. A., *Chem. Res. Toxicol*. 2001, *14*, 243 – 263.

[22] Lanni, J. S., Jacks, T., *Mol. Cell. Biol*. 1998, *18*, 1055 – 1064.

[23] Miller, B. M., Adler, I.-D., *Mutagenesis* 1989, *4*, 208 – 215.

[24] Pihan, G. A., Doxsey, S. J., *Sem. Cancer Biol*. 1999, *9*, 289 – 302.

[25] Oshimura, M., Barret, J. C., *Environ. Mutagenesis* 1986, *8*, 129 – 159.

